DYNAMIC NONLINEAR BENDING AND TORSION OF A CANTILEVER BEAM

THESIS

Michael S. Whiting, Captain, USAF
AFIT/GAE/ENY/06-M32

DEPARTMENT OF THE AIR FORCE
AIR UNIVERSITY

AIR FORCE INSTITUTE OF TECHNOLOGY

Wright-Patterson Air Force Base, Ohio

AFIT/GAE/ENY/06-M32

DYNAMIC NONLINEAR BENDING AND TORSION OF A CANTILEVER BEAM

THESIS

Presented to the Faculty

Department of Aeronautics and Astronautics

Graduate School of Engineering and Management

Air Force Institute of Technology

Air University

Air Education and Training Command

In Partial Fulfillment of the Requirements for the

Degree of Master of Science in Aeronautical Engineering

Michael S. Whiting, BS

Captain, USAF

June 2006

AFIT/GAE/ENY/06-M32

DYNAMIC NONLINEAR BENDING AND TORSION OF A CANTILEVER BEAM

Michael S. Whiting, BS
Captain, USAF

Approved:

Donald L. Kunz (Chairman)	date
Robert A. Canfield (Member)	date
Richard G. Cobb (Member)	date

Abstract

This effort sought to measure the dynamic nonlinear bending and torsion response of a cantilever beam. The natural frequencies of a cantilever beam in both chord and flap directions were measured at different static root pitch angles with varying levels of weights attached at the free end. The results were compared with previous experimentation to validate the data and testing procedures while lowering the associated error bands. Additionally, methodology for measuring mode shapes was set forth and mode shapes were measured for a few test cases with zero degrees of root pitch.

AFIT/GAE/ENY/06-M32

To My Loving Wife

Acknowledgments

I would like to express my sincere appreciation to my faculty advisor, Dr. Donald Kunz, for his guidance and patience throughout the course of this thesis effort.

Michael S. Whiting

Table of Contents

Page

List of Figures

List of Tables

List of Symbols

d_A = distance from A section mass center to weight mass center (in)

d_B = distance from B section mass center to weight mass center (in)

d_S = distance from solid section mass center to weight mass center (in)

I_{xx} = moment of inertia about the x-axis (lb-in^2)

I_{yy} = moment of inertia about the y-axis (lb-in^2)

I_{zz} = moment of inertia about the z-axis (lb-in^2)

L_A = length A section (in)

L_B = length B section (in)

L_S = length solid section (in)

M_A = mass of A section (lb)

M_B = mass of B section (lb)

M_S = mass of solid section (lb)

R_{iA} = inner radius of A section (in)

R_{iB} = inner radius of B section (in)

R_{iS} = inner radius of solid section (in)

R_o = outer radius (in)

VPP = volts peak to peak

DYNAMIC NONLINEAR BENDING AND TORSION OF A CANTILEVER BEAM

I. Introduction

Princeton Beam Experiment

In 1975 Dowell and Traybar performed a series of experiments looking into the dynamic and static responses of rotor blades undergoing flap, lag, and twist deformations. This series of test is more commonly referred to as the Princeton Beam Experiment. The experiment was funded by the U. S. Army Air Mobility Research and Development Laboratory, Ames Research Center in order to "support the validity [of]… nonlinear structural theory for rotor blade applications" [1:ii]. It was broken down into two parts, a static test portion and a dynamic test portion. In each portion, a cantilever beam was subjected to a tip load at various angles of root pitch. The beams were held in place and oriented at the various pitch angles by "a machine type, precision indexing-chuck" [1:4].

Static Tests

For the static portion of the experiment, three different size beams, made from 7075-T6 aluminum, were tested. The three beams were of the following dimensions:

Beam # 1 – 20″ by 1″ by 1/8″

Beam # 2 – 20″ by 1/2″ by 1/8″

Beam # 3 – 30″ by 1/2″ by 1/8″

Each was loaded with a series of weights at varying blade root pitch angles. Deformation measurements were made relative to the unloaded state. The planar deflections were determined by projecting the beams' images onto graph paper. The twist throughout the beams was measured by affixing lightweight rods along the length of the beams and measuring differences in rod positions relative to the unloaded cases and each other. The static measurements were only made for conditions at the blade tip.

Dynamic Tests

The dynamic portion of the experiment sought to characterize the behavior of the first natural frequency of a blade loaded beyond the linear range. For this portion of the experiment only beams #2 and #3 were tested. Each beam was set at the desired root pitch angle, with the desired load and excited by finger in either the flapwise or chordwise direction. The measurements were made by using strain gages mounted at the blade root and "in the proper orientation to be utilized as frequency transducers" [1:3]. The frequency data was then recorded as sinusoidal waves by "direct-writing, recording-oscillographs" [1:3] with a 60 Hz time reference signal. The time data and reference signal were then used to determine the response frequency by measuring the peak-to-peak time interval using the 60 Hz signal as the temporal reference. The dynamic data from beam #3 is provided in Appendix A for reference.

Comparison to Theory

The resulting static and dynamic data was compared to both conventional linear theory and a nonlinear theory developed by Hodges and Dowell. The value for the modulus of elasticity, shear modulus and Poisson's ratio were altered from "handbook

values" [3:542] in order to match the no tip weight load conditions. The comparison values used for the theoretical model are compared to the published values in Table 1.

Table 1 Material Property Differences Between Published Values and Those Used for the Nonlinear Theory Data Comparison

Variable	Published Value [4]	Comparison Value [3:542]	Difference (%)
Modulus of Elasticity	10,400 ksi	10,576 ksi	1.61
Shear Modulus	3900 ksi	4038.3 ksi	3.55
Poisson's Ratio	0.33	0.31	6.45

The result of the comparison was that the experimental data matched the nonlinear model substantially better than the linear model.

Follow-on Experimentation

A follow-on experiment was funded by the U. S. Army Air Mobility Research and Development Laboratory. This follow-on experiment looked exclusively at the static response of beam #2 from the original experiment. The effort sought to greatly improve upon the accuracy and data volume from the first test series. In this case static deflection data was taken at multiple points along the beam, instead of just the at the tip. No further dynamic data was taken.

Application

In order to validate complex beam theories and computer models, comparisons must be made to experimental data. Rotor blade models are used for numerous applications from design to damage analysis and life cycle modeling. In all cases the accuracy of the model is crucial to the success of its application. An inaccurate design model is likely to lead to either an overly robust system with a higher than necessary production cost or an inadequate one which can lead to a costly redesign effort. The

consequences of poor life cycle models are either earlier than needed part replacement, driving up long term system costs, or later than necessary part replacement, possibly leading to operational failures. The best way to validate the accuracy of a model is to apply it to experimental data. "For many years, a standard of comparison for nonlinear beam static and dynamic response has been the 'Princeton Beam' experiment" [2].

Limitations

The Princeton Beam Experiment had three substantial shortcomings. First, the experimenters failed to adequately document their set-up, making it difficult to model or reproduce. Second, the selection of data points was somewhat inconsistent, limiting the usefulness of the collected data. For instance, the dynamic response of the 30″ beam at 35 degrees pitch with a one pound load was only measured in the chordwise direction and not the flapwise direction, and the 30″ beam dynamic response was measured at pitch increments of five degrees for the two pound load and 10 to 15 degree increments for the one pound load. Third, the error analysis was inconsistent with the collected data. The report claims an error in frequency determination which is considerably smaller than that which shows up in the measured data when multiple readings were taken with identical set-ups.

Research Objectives

The purpose of this experiment is to serve as an update to the dynamic portion of the Princeton Beam Experiment and validate testing methodology for future experimentation.

This experiment will improve upon the accuracy and extent of the Princeton Beam experiment by using more modern technology and methodology. Whereas Dowell

and Traybar were only able to find the first natural frequency in the flapwise and chordwise directions, this experiment will explore higher order modes and will characterize the shape of those modes through the use of a laser vibrometer. Additionally, the experimental apparatus' will be sufficiently documented so as to remove the guess work from future modeling.

Follow on experimentation has been planned which will incorporate more complex materials and geometry; therefore it is imperative that the testing methodology provides accurate results. In order to validate the testing methods used, the resultant data will be compared to the data from Princeton Beam Experiment whenever possible. Where Princeton Beam data is not available comparison to theoretical results will be used for validation.

II. Methodology

Parts Fabrication

Since experiment was designed to reproduce the results found by Dowell and Traybar and use them as a base line for comparing results and the validity of the testing methods, the set-up and parts manufacturing sought to match their experiment to the maximum extent possible.

Beams

Two beams were manufactured with the same specifications laid out in the Princeton Beam Experiment, using the two sets of dimensions which had been tested for dynamic data. Both beams were manufactured out of 7075-T6 aluminum and had the following dimensions:

Beam #1 – Length 24″ (20″ of cantilever), Width ½″, Thickness 1/8″

Beam #2 – Length 34″ (30″ of cantilever), Width ½″, Thickness 1/8″

Beam #1 was visibly warped during manufacture and was deemed unusable for experimentation, a subsequent beam of the same dimensions was manufactured to replace it, but this beam also warped during manufacture, leaving only beam #2 fit for experimentation. The center of the tip of each beam was tapped ¼″ along the long axis to accommodate the 1/16″ diameter attachment screw.

Tip Weights

The tip weight descriptions from the Princeton Beam Experiment were too vague to be confidently replicated; therefore, it was left to the experimenter to determine the

best method for designing and fabricating the weights. A cylindrical weight design (similar to that indicated by Dowell and Traybar) was selected in order to simplify any modeling of the weights. Each weight was cut from one of three separate solid steel rods, The rods differed in diameter with values of 2″, 3.5″, and 4″. The particular rod used for each weight was chosen so as to minimize the variation in lengths. Each weight was designed with a ¼″ long solid section with a 1/16″ hole for accommodating the attachment screw, with the remainder of the weight having a .516″ bore. The solid section was located longitudinally off-center so that when attached to the beam, the center of mass of the weight would be located at the tip of the beam as shown in Figure 1.

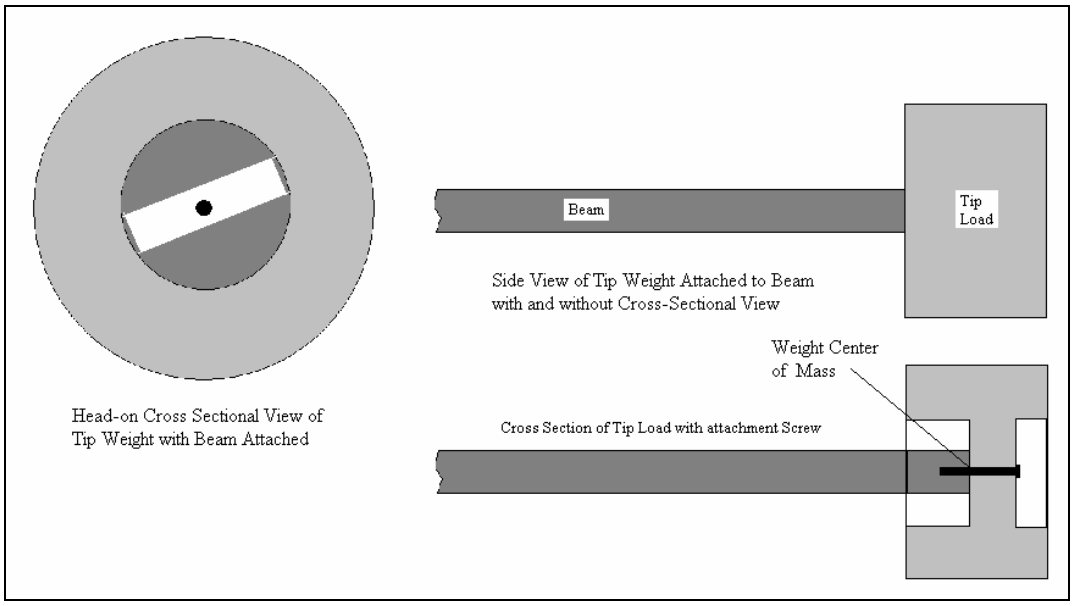

Figure 1 Weight Cross Sections

This was done by drilling a separate .516″ hole from either side of the beam. Table 2 shows the nominal weight dimensions, with bore A being the beam side of the weight and bore B being the free side of the weight.

Table 2 Tip Weight Dimensions

Designed Weight (lb)	Diameter (in)	Total Length (in)	Bore A Length (in)	Bore B Length (in)	Actual Weight (lb)
0.5	2	0.939	0.633	0.056	0.49
1	2	1.158	0.588	0.320	1.01
1.5	2	3.471	1.899	1.322	1.50
2	3.5	0.727	0.366	0.111	2.01
3	3.5	1.094	0.550	0.294	3.02
4	4	1.112	0.733	0.129	4.01
4.5	4	1.251	0.824	0.177	4.52

The 0.5 and 1.5 lb weights were manufactured for a wider beam with 1.505″ diameter bores, but were otherwise identical in nature to the rest of the weights, which are depicted in Figure 2.

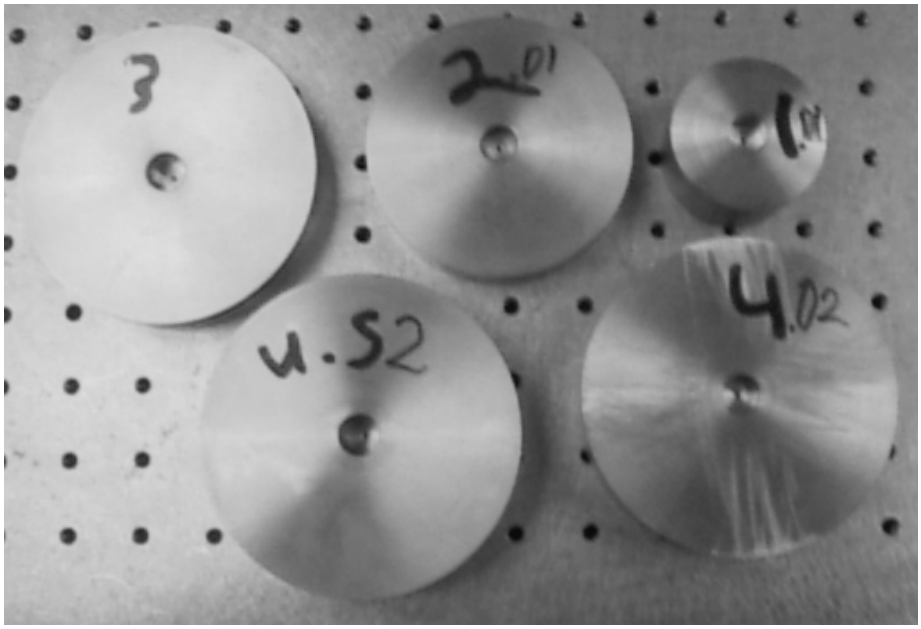

Figure 2 Tip Weights

The weights were fixed to the beam using a 1/16″ screw.

Each weight's moments of inertia were calculated using the following equations:

$$I_{xx} = \tfrac{1}{2}*M_A*(R_{iA}^2+R_o^2) + \tfrac{1}{2}*M_B*(R_{iB}^2+R_o^2) + \tfrac{1}{2}*M_S*(R_{iC}^2+R_o^2) \quad (1)$$

$$I_{yy} = I_{zz} = 1/12*M_AL_A^2+M_A*d_A^2 + 1/12*M_BL_B^2+M_B*d_B^2 + 1/12*M_SL_S^2+M_S*d_S^2 \quad (2)$$

Figure 3 shows the general geometry breakdown of the weights used for the moment of inertia calculations.

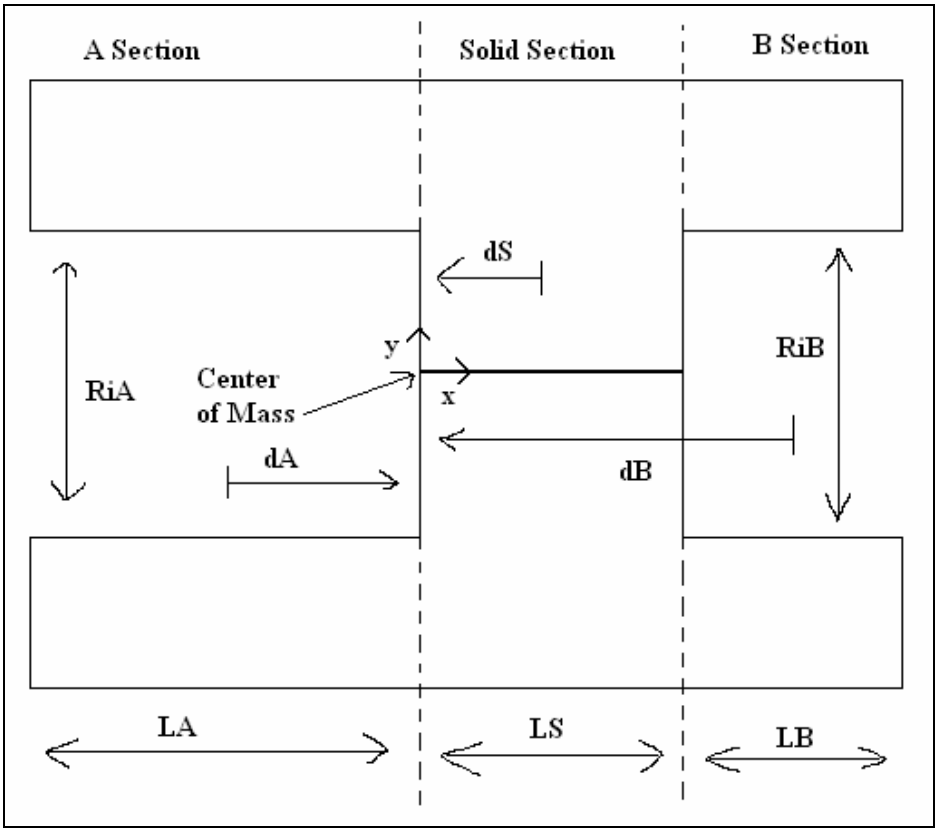

Figure 3 Moment of Inertia Equation Variables

Using the axis of symmetry as the x-axis, the moments of inertia for each weight has been calculated about the center of the tip of the beam, with the results listed in Table 3.

Table 3 Moment of Inertia Calculations

Weight (lb)	I_{xx} (lb-in^2)	I_{yy} (lb-in^2)
0.49	0.345	0.048
1.01	0.531	0.112
1.50	1.142	1.538
2.01	3.122	0.088
3.02	4.702	0.300
4.01	8.124	0.537
4.52	9.160	0.765

Set-Up

The beam was clamped to the swivel attachment with a cover plate and four ¼″ diameter bolts, so that 30″ of beam extended past the clamp point. The swivel attachment was then bolted to a rod fixture using two ¼″ diameter bolts. The rod fixture was clamped to a fixation rod with two ½″ diameter bolts. The fixation rod was bolted in place on a vibration isolation table by four ¼″ diameter bolts. This set-up can be seen in Figure 4 for the zero degree pitch case.

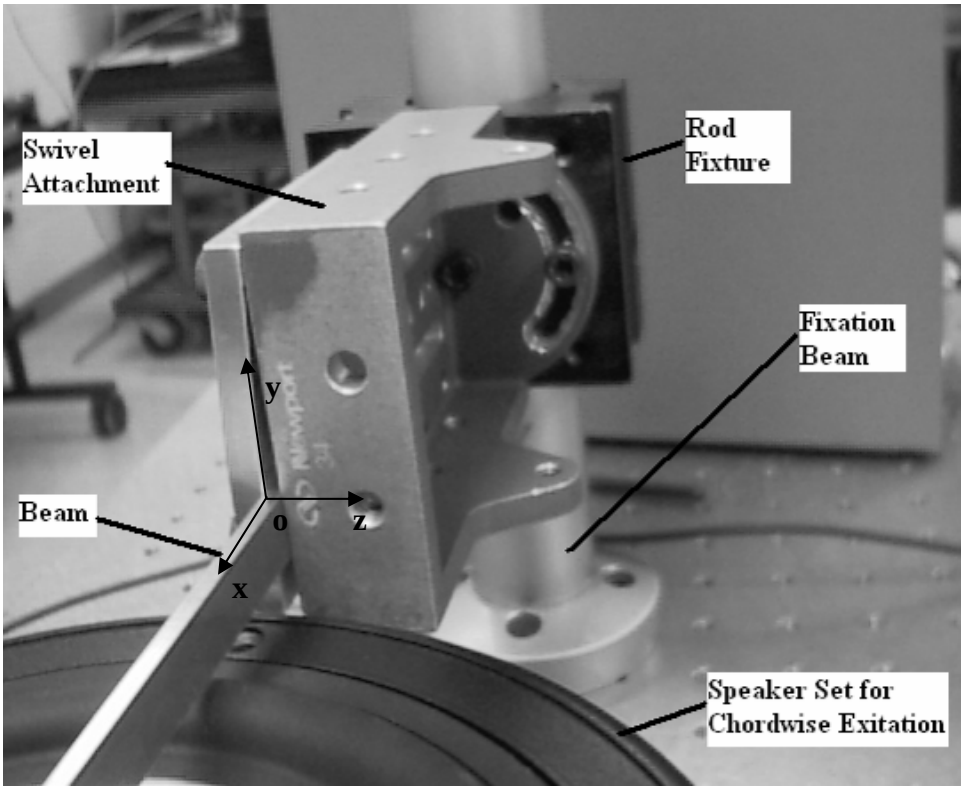

Figure 4 Swivel Attachment

The swivel attachment allowed for 360 degree pitch rotation of the beam between trial runs, while fixing the beam in place for each trial. The base of the beam where it attaches to the swivel attachment is considered the origin, with positive length measurement going

toward the end of the beam where the tip weights attach. The directional and pitch terminology is shown in Figure 5.

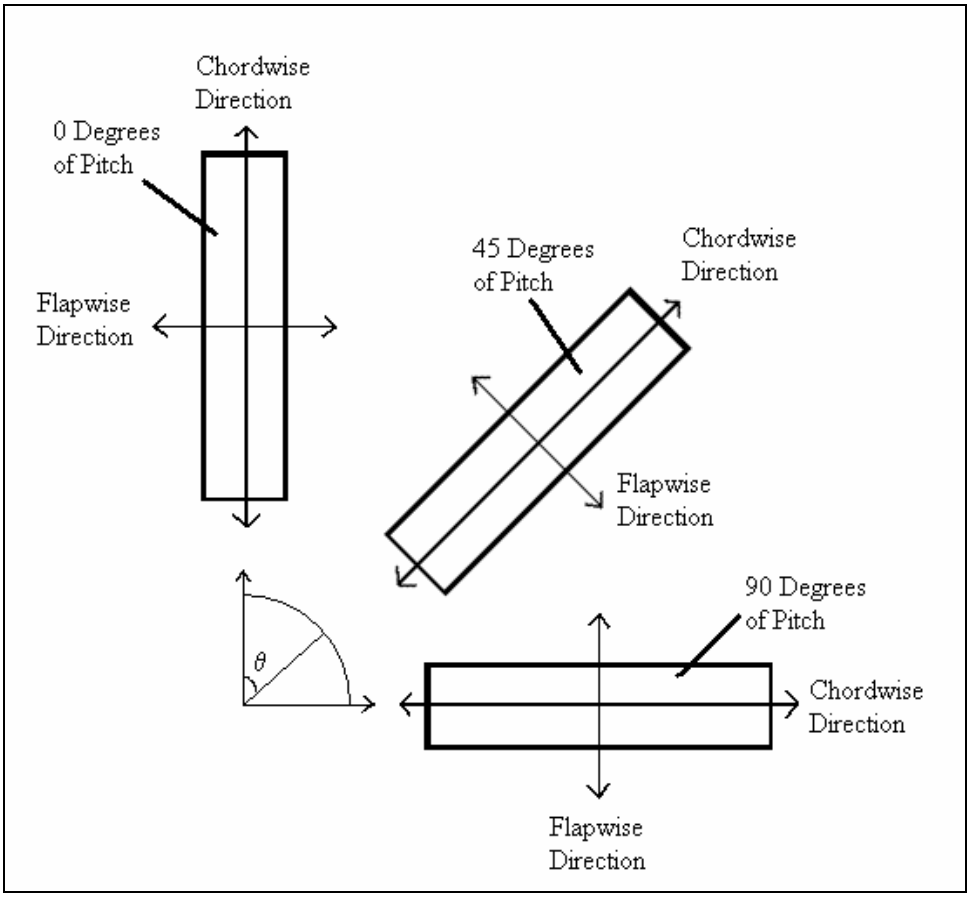

Figure 5 Directional Orientation

The pitch angle was set and measured using an SPI Protracto Level II Inclinometer. Pitch angle refers to the beam pitch angle at the root where it is held by the swivel attachment.

Accelerometers

For the frequency determination portion of the experiment, an accelerometer was mounted in each of three locations. Each accelerometer was a PCB Piezotronics model number 352C22, weighing 0.5 grams (0.0011 pounds). The combined weight of the accelerometers was only 1.8% of the unloaded beam weight (0.182 lb) and less than 0.5%

of the lowest loaded beam weight, making their contribution negligible. One was placed at 28″, centered on the wide side of the beam to measure the flapwise frequency. One was placed at 28.25″, off-center on the wide side of the beam to measure the flapwise frequency and identify/eliminate rotational frequencies. One was placed at 29″, centered on the narrow side of the beam to measure the chordwise frequency. This arrangement is illustrated in Figure 4.

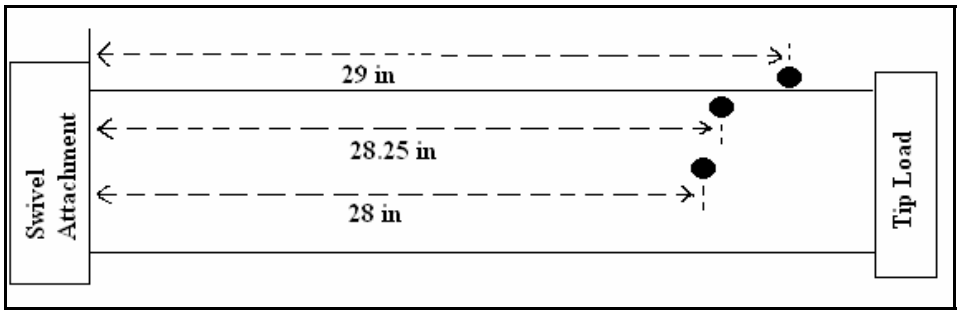

Figure 6 Accelerometer Locations

The beam was manually excited simultaneously in the flapwise and chordwise directions. This was done by striking the beam off center at the midspan by finger, simulating an impulse force. The accelerometers were attached to a SignalCalc Savant Dynamic Signal Analyzer operating with SigCalc 720 software which used a Fourier Transform routine to convert the time data into frequency data. The natural frequencies were identified in the frequency domain by large rises in output value. The software was set to average 5 data sets with a 90% overlap, a frequency span of 20 Hz (40 Hz sampling rate), a time span of 160 seconds, and a Hanning window. These settings allowed for a measurement accuracy of +/-0.0038 Hz in the flapwise direction and +/-0.0084 Hz in the chordwise. By contrast, the Princeton Beam Experiment at best allowed for a frequency measurements accuracy of +/-0.1012 Hz in the flapwise direction and +/-0.0617 Hz in the

chordwise. During this portion, only the first natural frequency was recorded for each direction (flapwise and chordwise).

Laser Vibrometer

For the mode shape portion of the experiment, the Polytec Scanning Vibrometer PSV 400-3D with software version 8.2 was used to measure velocity data which was then converted into normalized mode shape data. Hi-Vi Research Model F6, 60 Watt, 8 ohm speaker was used to excite the root end of the beam in the desired direction. To create steady state data, the speaker was set to excite the beam at the specific frequency of interest and allowed to act on the beam for several minutes prior to scanning. The speaker input amplitude was set to ten volts-peak-to-peak (VPP) for frequencies below 10 Hz and 5 VPP for frequencies above 10 Hz. The laser vibrometer scanned the beam, measuring velocity values at each of 25 predetermined points along the neutral axis, and combined this data with the input signal to the speaker to record phase and peak velocity data at the desired frequency. The velocity and phase data was then used to plot the mode shapes. This set-up is depicted in Figure 7.

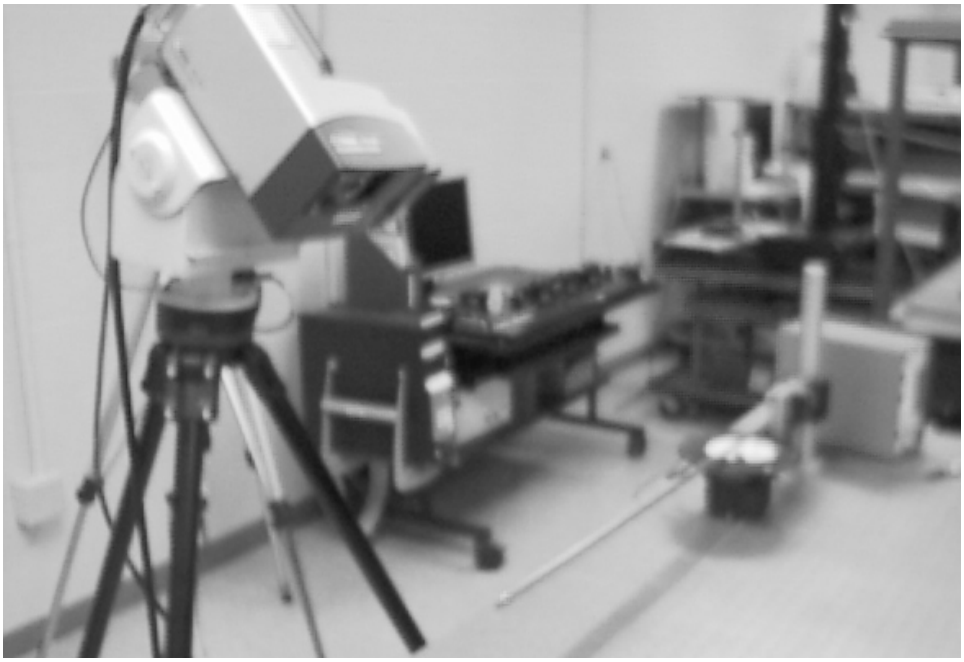

Figure 7 Scanning Laser Vibrometer Set-up

Attempts were made at creating two and three dimensional grids; however, this could not be done for a sufficiently large portion of the beam due to limitations of the laser vibrometer, unavailable static measurements and the length/slenderness ratio of the beam. Specifically, the 60 to 1 length to height ratio forced the camera to be zoomed out to the point where automatic alignment for multi-dimensional grids was not possible as the minimum separation between alignment points forced them to be separated by more than the width of the beam. Manual alignment of the equipment for multi-dimensional grids requires exact static measurements of the loaded system. The unavailability of this data eliminated manual alignment as an option. Consequently, only the one dimensional measurements were made.

The scanning laser vibrometer was also used to determine higher order natural frequency values in the chordwise direction. For these tests the desire was only to identify the desired frequencies and then use the previously mentioned set-up to

determine the mode shapes. The set-up was similar to that described above, with a few differences intended to either decrease testing time or allowing for frequency identification over a range of values. First, the speaker was set to excite the beam over a large range of frequencies (0 to 256 Hz), rather than just the desired frequency. Second, only five scan points were used, this significantly decreased the testing time while only eliminating mode shape data which would be captured in subsequent testing. Last, the laser vibrometer software was set to display the frequency response of the system using a Fourier transform routine which was then used to identify the second and third natural frequencies.

Instrumentation Choices

The laser vibrometer was initially considered the preferred data collection method due to its ability to collect data along the entire length of the beam; however, it has three limitations which necessitated the use of accelerometer measurements. First, the laser vibrometer software limits open frequency scan resolution to +/- 0.0156 Hz. Since the first natural chordwise frequencies occur below 1 Hz, this leads to measurement errors as great as 14% for the first mode; whereas, the accelerometers allowed for the determination of the natural frequencies to within +/- 0.0038 Hz (0.05-0.77% chordwise error, 0.09-1.41% flapwise error). Second, once pitch is introduced, the set-up requirements become extremely time consuming and the laser has a hard time reflecting back to the vibrometer. Third, geometrical angle limitations coupled with the narrow width of the beam made it impossible to acquire flapwise frequency data along the entire beam length in a single trial run.

III. Results and Analysis

Differences in Methodology

A few differences in techniques and methodology may contribute to the small differences in data recorded in this experiment versus the Princeton Beam data. Dowell and Traybar claim to have an error in frequency reading of only +/-0.1% [1:5], however in several cases multiple readings were taken for the same set-up with a difference in measurement as high as 2.53% and they made no allowance for instrumentation error or repeatability error. Additionally, the fixture holding the beam root used by Dowell and Traybar could not be reproduced, so a different one described previously was used. The Princeton Beam Experiment documentation lists all load weights as whole number values and all angle measurement are listed as exact whole numbers in five degree increments, with the precision of these measurements left unknown. The new data is taken with an angle measurement precision of 0.1 degree and a weight measurement precision of 0.01 lb. Additionally, the angle setting limitations of the swivel attachment made getting closer than one degree to a desired angle very difficult; producing some small differences in data points. The Princeton Beam data was derived from measurements taken at the blade root, rather than the blade tip which increases the associated precision error as a result of the smaller amplitudes for the first natural frequency. Finally, the instrumentation used in the Princeton experiment consisted of glued-on strain gages (circa 1975) which introduces more stiffness than the lightweight accelerometers used in

this experiment; thus causing a small, but not necessarily inconsequential increase in the measured frequencies.

Error Calculations

While several factors can contribute to error in this kind of experiment, the greatest known sources present in the experiment were those caused by frequency resolution limitations and the instrument sensitivity. The frequency resolution limitations result from digitizing the data; whereby, the measured frequency readings were separated into discrete values, not continuous ones; the true value actually lies closest to the reported number, but is possibly higher or lower by an amount based on the frequency resolution. The frequency resolution is found by taking the reciprocal of the sampling time. For the new data this resolution is +/-0.0063 Hz. The instrument error associated with the accelerometers as stated by the manufacturer is +/-0.002 Hz in the range under consideration. Repeatability error is another error concern. This error type is introduced when slight differences in set-up occur for identical test cases. One source of such error was that the degree to which each swivel attachment bolt was tightened was not measured and may have varied. Repeatability error for this experiment will be defined as the maximum change in recorded value for identical test cases and will be separated between flapwise and chordwise orientations. This leads to a repeatability error of +/-0.000 Hz in the flapwise direction and +/-0.0130 Hz in the chordwise direction. Using the same technique, the repeatability error for the Princeton Beam Experiment was +/-0.1430 Hz in the flapwise direction and +/-0.0870 Hz in the chordwise direction. Combining these sources of error by the root mean squared method shown in Equation (3) leads to an error of +/-0.0038 Hz in the flapwise direction and +/-0.0084 Hz in the chordwise direction.

$$E = ((e_1^2 + e_2^2 + \ldots e_n^2)/n)^{1/2} \quad (3)$$

Where

E = total error

e_i = error from source number i

n = total number of error sources

The resultant Princeton Beam Experiment error is +/-0.1012 Hz in the flapwise direction and +/-0.0617 in the chordwise direction. The resulting decrease in error band size has been demonstrated in Figure 8.

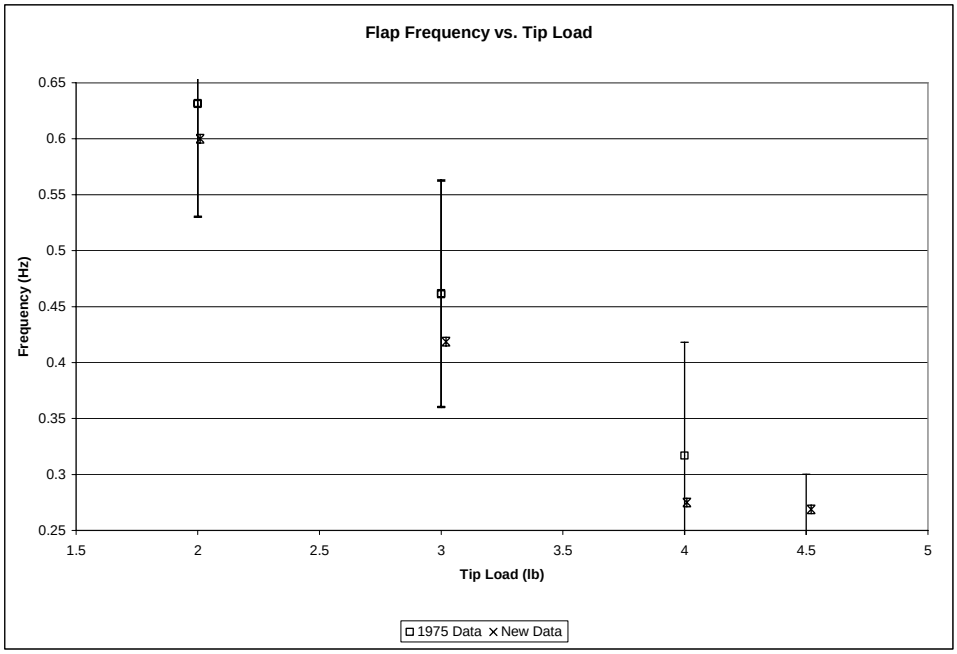

Figure 8 Reduction in Error Bands

As for the velocity measurements, the only source of error came from the precision limitations of the laser vibrometer and associated software. The manufacturer lists this error as no more than 1%.

Natural Frequencies

The first natural frequencies of the beam in the flapwise and chordwise directions were determined using the accelerometer set-up. Higher order natural frequencies were measured using the laser vibrometer for the zero degree pitch angle case, with zero, one, two, and three pound loads.

The general trend for flapwise natural frequency is demonstrated in Figure 9 where the frequency increases in a nonlinear manner as pitch angle increases, eventually maxing out by 80 to 90 degrees of pitch.

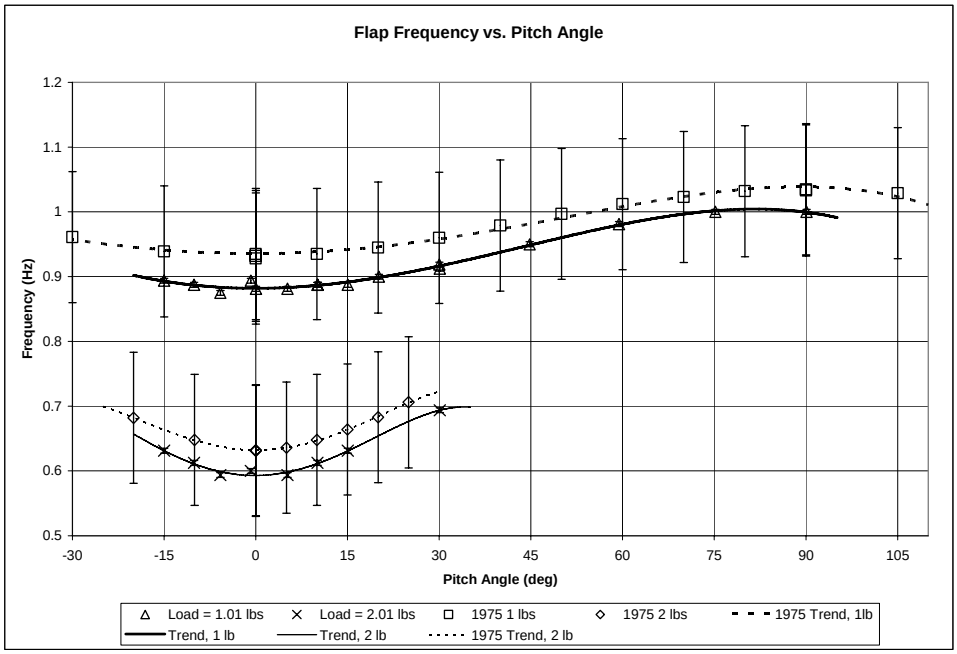

Figure 9 Flapwise Frequency vs. Pitch Angle

Figure 9 also shows the error bands for the newly collected data and for the 1975 data. The 1975 data clearly allows for the variation in frequency merely being a matter of measurement error, while the new data definitively demonstrates the existence of the frequency dependence on pitch angle. Additionally, the new data is soundly inside of the

error bands from the Princeton Beam Experiment and follows the same trend, providing a high degree of confidence in the results.

The general trend for chordwise natural frequency is demonstrated in Figure 10 where the frequency decreases in a nonlinear manner as pitch angle increases, reaching a minimum between 80 and 90 degrees of pitch.

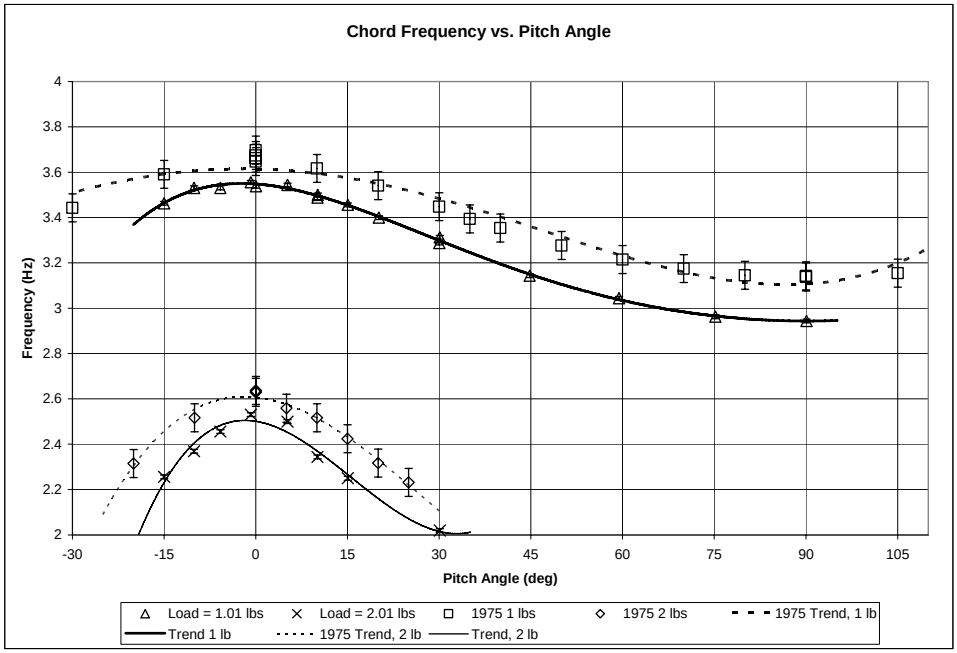

Figure 10 Chordwise Frequency vs. Pitch Angle

These trends in frequency versus pitch angle match the Princeton Beam Experiment and remained consistent for all tip weight values. It is notable that the new data falls outside of the error bands from the Princeton Beam Experiment. Part of the reason for this is that the error bars from the Princeton Beam experiment have been made estimates of the error 30 years after the experiment was performed and those estimates represent absolute minimums and are likely to be smaller than the true error bars. Additionally, differences in methodology previously mentioned have contributed to a small difference in the

solution, specifically, the stiffening affect of the strain gages in the Princeton Beam Experiment and failure to account for the presence of higher order modes raised the measured values with respect to the uninstrumented (true) values.

It should be noted that in both the flapwise and chordwise directions the new measurements average 5.7% lower (standard deviation of 3.3%) for the same test conditions. This disparity is mostly likely the result of the differences in experimental set-up mentioned previously. Additionally, the small changes in pitch angle used for test points can have a significant impact on the frequencies for the heavy tip loads. Specifically, when the 4.5 lb weight was applied with -0.8 degrees of pitch, the total twist of 17 degrees is reached by the end of the beam; on the other hand, a zero degree pitch should have resulted in no twist at all. This is a large part of the reason why the 4.5 lb weight registered a noticeably higher flapwise frequency than the Princeton Beam Experiment.

When the frequency changes are tracked versus tip load, the result is a nonlinear decrease which closely matches the results found in the Princeton Beam Experiment. A comparison of the new data with the 1975 data for frequency vs. tip load can be found in Figure 11 and Figure 12.

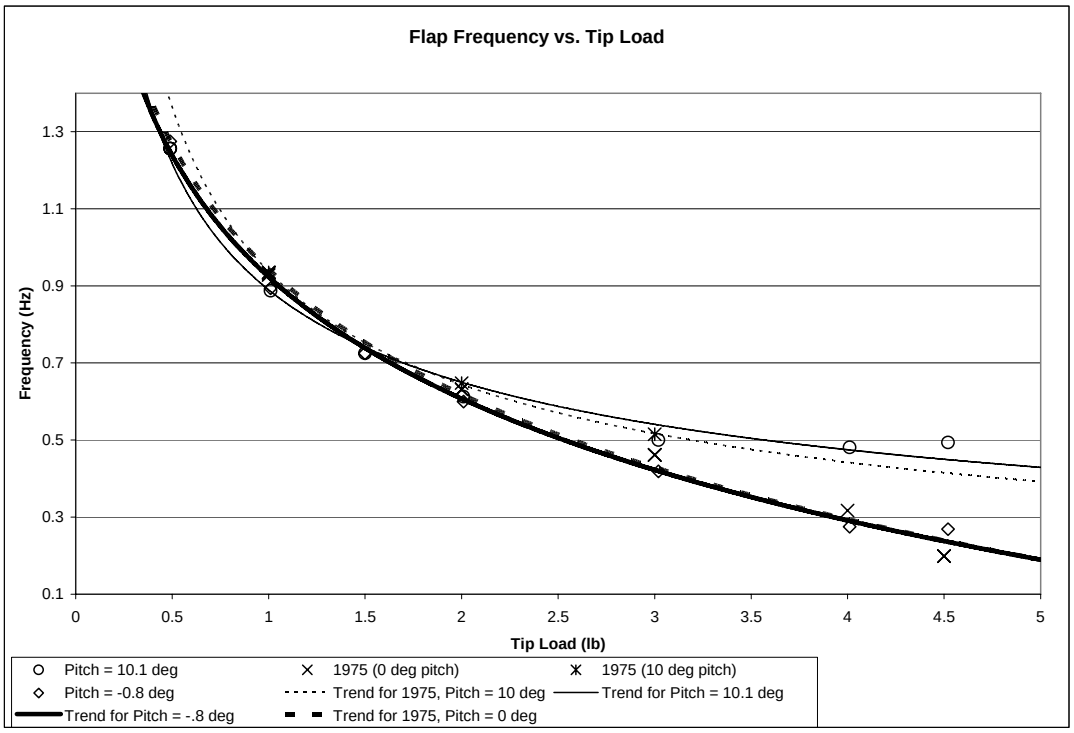

Figure 11 Flapwise Frequency vs. Tip Load

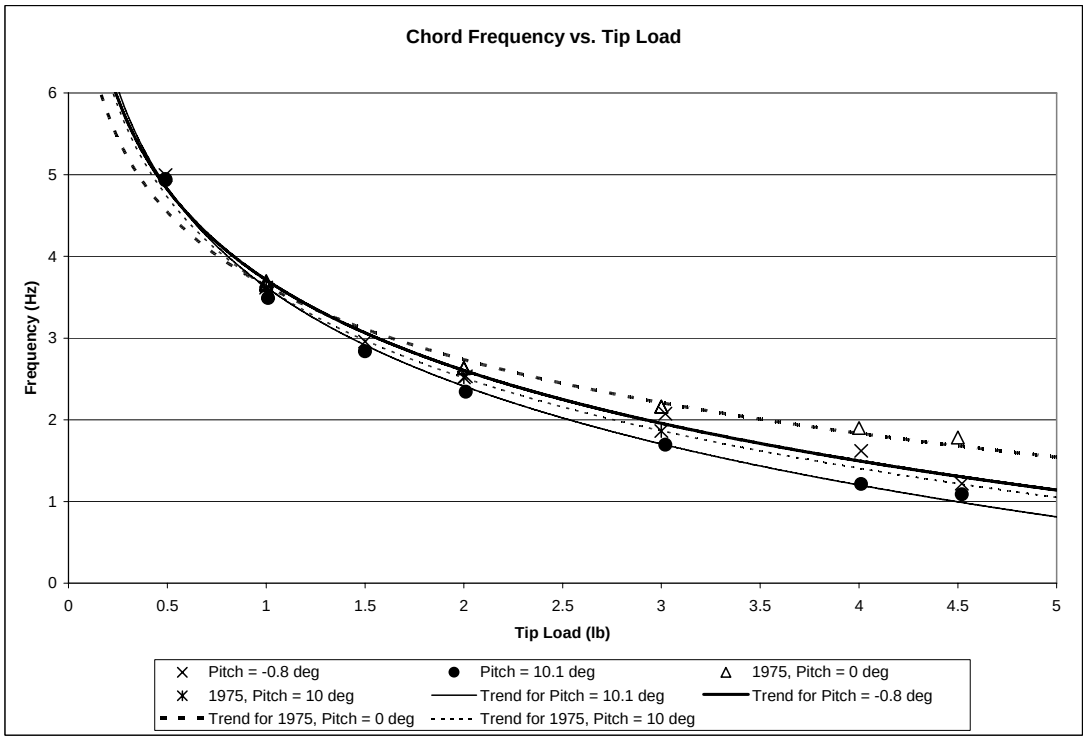

Figure 12 Chordwise Frequency vs. Tip Load

Trend lines have been added to the figures to simplify the comparison. The trend lines use a power series method to determine a line which most closely matches the associated data, these lines are not necessarily the correct equations for the experimental set-up, rather they represent data matching and are used for comparison purposes only.

Mode Shapes

Consistent mode shape data was only obtainable in the flapwise direction at 0 degrees pitch. The data was taken by recording the peak velocity output at known locations on the beam centerline and normalizing it. The beam length was normalized by dividing the data point length coordinate by the total beam length (x/L). The velocity data was normalized by dividing the velocity recorded at each data point by the maximum velocity recorded for the mode shape in question, so that the peak value becomes +/-1. Since acceleration, velocity and displacement data differ only by constant multipliers, dependent on the test frequency, the normalized data can be interpreted as representing the displacement, velocity, and acceleration variation along the beam. The Princeton Beam Experiment did not seek to identify mode shape data; therefore, the data will be compared to linear theory as, developed in Appendix B, to show general form agreement, recognizing that the reason experimental data of this nature is needed is that linear theory cannot be applied to the high load limits of rotor blades. The linear theory results will be calculated at the zero pound load case and the infinite pound load case. The infinite load case represents the solution with a tip load weighing 10^{11} pounds which while not truly infinite, is sufficiently large compared to the beam weight as to approximate an infinite load case.

Figure 13 depicts the first mode shape as compared to linear theory.

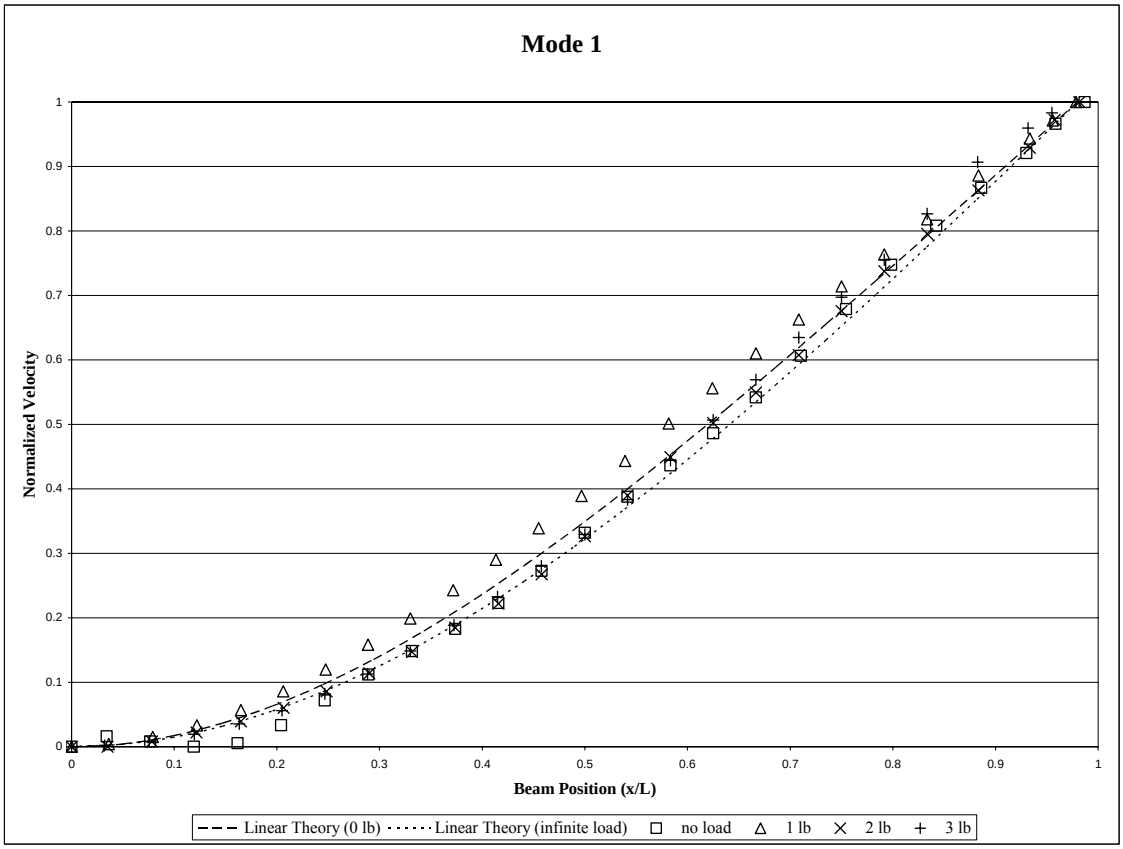

Figure 13 Flapwise Mode 1

It is evident that for this particular set of weights and zero pitch, that linear mode shape theory predicts the correct approximate shape for the first mode. This is not surprising in that the data has been normalized to a maximum magnitude of one and the primary difference for the first mode from the linear to the nonlinear range should be their relative magnitude.

The second mode shape also closely matched linear theory as shown in Figure 14.

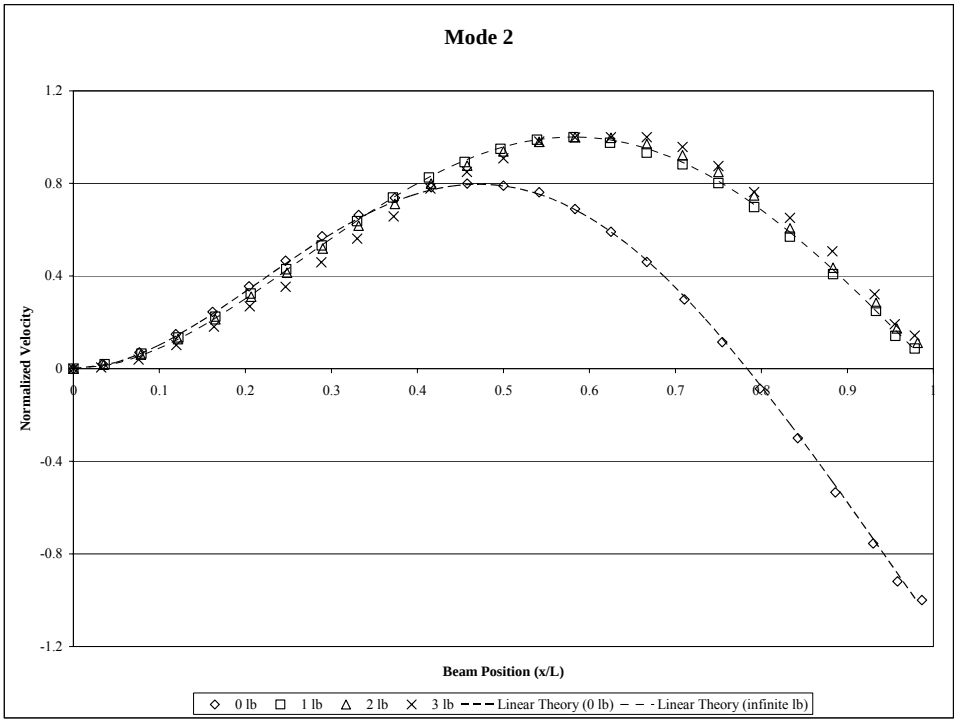

Figure 14 Flapwise Mode 2

The most notable change that the tip loads have caused is to push the node out to the right, so that it is predicted to occur just beyond the end of the beam, rather than at 78% of the beam length as with the no load condition. Also, the change in tip load has caused virtually no change in mode shape. This is because the lowest test weight is sufficient to change the mode so as to match the infinite load condition; had smaller weights (inside of the linear range) been used, there would have been intermediate mode shapes lying between the no load line and the 1 lb load line.

With the third mode shape, the regularity of the results no longer holds. Figure 15 clearly demonstrates a distinct shape for each test condition, ones which are no longer predicted by linear theory.

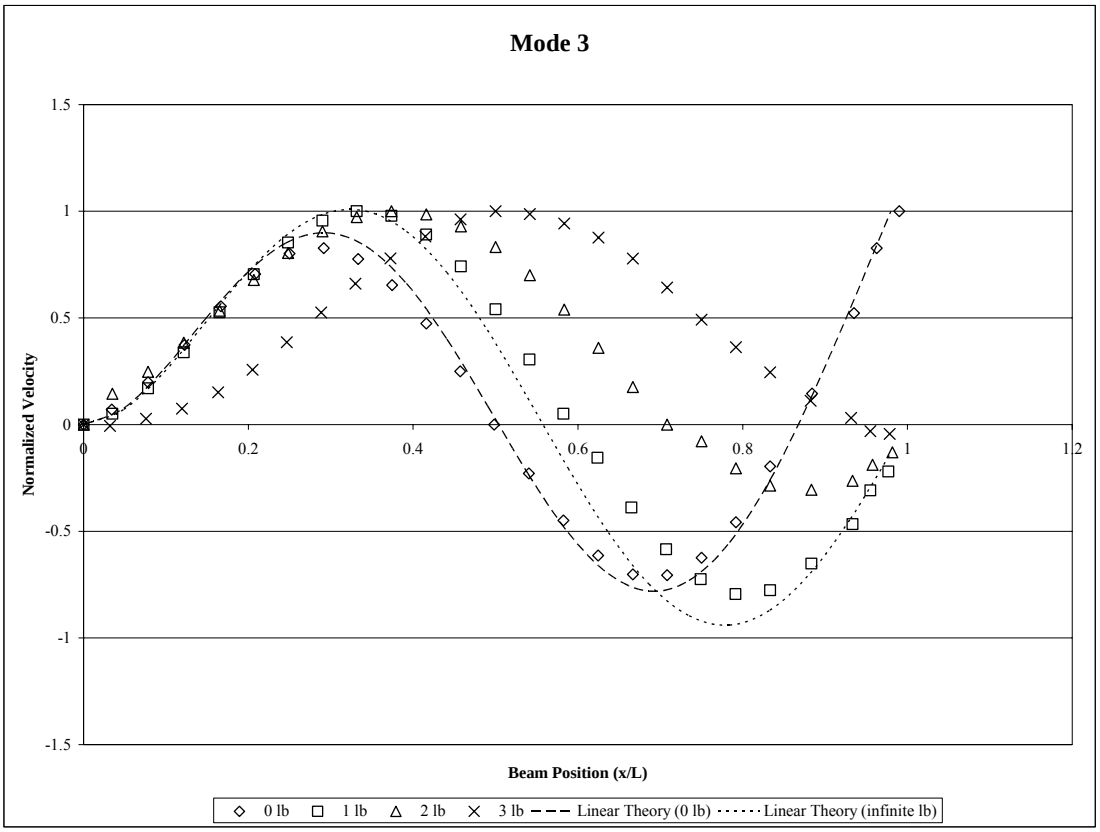

Figure 15 Flapwise Mode 3

For each tip load case, the nodes have both been shifted rightward. In fact, with the three pound weight, the second node has almost shifted to the end of the beam. A large part of the reason for the rightward shift in the node locations is that the tip load at the end of the beam is significantly heavier than the beam itself. Even the 1 lb load is 5.67 times the weight of the beam. As a result of the weight disparity, the tip loads act as inertial dampers, attempting to keep the end of the beam from moving at the higher frequencies. Thus the beam with the heaviest load acts like a fixed-fixed beam excited at the first mode, rather than a cantilever beam excited at the third mode. This inertial damping effect is not accounted for by linear theory.

IV. Conclusions and Recommendations

Accelerometer Results

The accelerometer results greatly improved upon those of the Princeton Beam Experiment. The natural frequency results fell within the error bands from the Princeton Beam Experiment and the error band sizes were reduced by an order of magnitude. This data used time averaging of several overlapping tests while the Princeton Beam Experiment used singular test results. The beam instrumentation accounted for the presence of higher order modes and separated them from the desired modes while the Princeton data makes no allowance for higher order modes. The new data points were selected at equal angular increments for each load case, making it more useable than the prior data. The experimental process has been sufficiently documented as to be replicated and modeled by others, which was the greatest shortcoming of the Princeton Beam data. All the natural frequency data collected followed the same trends and fell within the limits established by past experimentation while at the same time reducing several sources of error, making the data more reliable than the Princeton Beam Experiment data.

Laser Vibrometer Results

There is no baseline of comparison for the laser vibrometer results. This experiment was performed to measure mode shapes outside of the linear range and no similar experimentation has been identified. Complex nonlinear models were not available for comparison. This is the reason that measurements were taken for the

unloaded case as well as the loaded cases. The unloaded results match closely with theoretical results which have been validated and documented in numerous texts. Since the experimental process used for both unloaded and loaded cases was identical, the results from the loaded cases are at least as good as the unloaded results. The mode shapes graphed in the results sections accurately reflect the actual mode shapes experienced by the beam.

Laser Vibrometer Evaluation

The laser vibrometer use was limited by a number of problems which may be avoidable in future experimentation. The greatest limitations were related to frequency resolution, beam geometry, deformation extent, and a lack of static data. At the same time it provided a great deal of data which could not have otherwise been obtained.

Frequency Resolution

The laser vibrometer used for this experiment is limited to a frequency resolution of +/-0.01562 Hz while scanning to detect natural frequency values. For this particular experiment, the resulting error in measured natural frequencies would have been as great as 5.8% and averaged 2% in the flapwise (worst case) direction. On the other hand, the accelerometer set-up has no such resolution limit and can be made to measure with as fine a resolution as desired; however, the trade off is an ever increasing experimental time required to meet the desired resolution. For simplicity, the same settings were used for all accelerometer tests; these settings led to a maximum frequency error of 2.3% and average error of 0.7% for the flapwise direction. Table 4 shows the minimum frequency value detectable for a given maximum desired error for both the laser vibrometer and the accelerometer (as used in the experiment). What this amounts to is that the laser

vibrometer is not very accurate in determining natural frequencies below 1.25 Hz. For future considerations, use of a beam which is shorter, more rigid, thicker, or otherwise designed to have a higher first natural frequency would allow for the entire experiment to be performed using only the laser vibrometer.

Table 4 Frequency Limitations

Laser Vibrometer Minimum Detectable Frequency (Hz)	Accelerometer Minimum Detectable Frequency (Hz)	Maximum Error (%)
6.25	15.625	0.1
1.25	3.125	0.5
0.625	1.5625	1
0.125	0.3125	5
0.0625	0.15625	10

Twist

The laser vibrometer requires that the laser beam be reflected back to the vibrometer in order for measurements to be made. With the 30″ beam used in this experiment, a tip load of one pound with a pitch of only ten degrees caused sufficient twist in the beam as to stop the laser from reflecting back to the vibrometer along large portions of the beam, making modal mapping impossible. In the future this problem may be avoidable with a structure that either twists less severely or a surface which provides better beam reflection.

Static Measurements

The laser vibrometer is capable of performing up a three dimensional analysis of a specimen; however, this requires a static mapping of the structure for each test case. Obtaining the static measurements for all test cases prior to dynamic testing would allow for the creation of substantially improved mode shape mapping.

Beam Geometry

The length of the beam required it to be placed two meters from the laser vibrometer in order to capture data along the entire length. This distance requirement, coupled with the narrow flapwise side of the beam and the need for reasonable beam angles, made it impossible to capture mode shape data in the chordwise direction. In fact, attempts were made to capture chordwise data along only half the length of the beam at zero degree pitch angle, but the 1/8″ surface proved too small to collect data over longer than a 2″ span in any single run. Using a shorter, thicker specimen in the future may make it possible to capture this additional information.

Benefits

There were several benefits to using the laser vibrometer. The laser vibrometer allowed for the relatively simple determination of mode shapes. Without this equipment, mode shapes would be virtually indeterminate. The laser vibrometer requires absolutely no instrumentation to be mounted on the test specimen; thus the specimen characteristics are left unaffected by the equipment. Accounting for the problems mentioned above would allow for the creation of a three dimensional model of a specimen which can determine the natural mode shapes and frequencies across a large spectrum range in a single scan.

Future Experimentation

Several matters presented themselves which would be of interest for future study. No torsional analysis was performed; however there was clearly a torsional element present, particularly with the heavier weights. The first torsional mode decreased by at

least one order of magnitude between the 1/2 lb load condition and the 4.5 lb load condition. The first torsional frequency also displayed a visible dependence on pitch angle. At the third mode shape, the beam was beginning to act more like a fixed-fixed beam than a cantilever beam; it would be interesting to determine if this continues to happen with higher order modes.

Ultimately, future experimentation would be greatly aided by using a specimen which is shorter, stiffer, thicker, and/or possessing of a first natural frequency of at least 1.25 Hz. Even without such adjustments, the experimental process laid out in this report lead to accurate measurements of natural frequencies and mode shapes for cantilever type beams.

Appendix A. Data

Table 5 Accelerometer Data

Trial #	Tip Load (lb)	Pitch (deg)	Flapwise Frequency (Hz)	Chordwise Frequency (Hz)
1	1.01	0.02	0.8812	3.538
2	1.01	10.14	0.8875	3.5
3	1.01	20.12	0.9	3.4
4	1.01	30.03	0.9187	3.288
5	0.49	-0.8	1.275	4.994
6	1.01	-0.8	0.8937	3.556
7	1.5	-0.8	0.725	2.956
8	2.01	-0.8	0.6	2.531
9	3.02	-0.8	0.4187	2.075
10	4.01	-0.8	0.275	1.619
11	4.52	-0.8	0.2688	1.219
12	0	-0.8	4.213	16.31
13	0	5.18	4.288	16.38
14	0.49	5.18	1.256	4.962
15	1.01	5.18	0.8812	3.544
16	2.01	5.18	0.5937	2.5
17	1.5	5.18	0.7187	2.938
18	3.02	5.18	0.4375	1.913
19	4.01	5.18	0.3875	1.338
20	4.52	5.18	0.4125	1.137
21	4.52	5.18	0.4125	1.144
22	0	-5.8	4.194	16.36
23	0.49	-5.8	1.256	4.975
24	1.01	-5.8	0.875	3.531
25	2.01	-5.8	0.5937	2.456
26	3.02	-5.8	0.45	1.881
27	4.01	-5.8	0.3937	1.388
28	4.52	-5.8	0.425	1.125
29	1.5	-5.8	0.7187	2.919
30	1.5	-10.1	0.725	2.819
31	0	-10.1	4.175	16.47
32	0.49	-10.1	1.25	4.95
33	1.01	-10.1	0.8875	3.531
34	2.01	-10.1	0.6125	2.369
35	3.02	-10.1	0.5	1.706

Trial #	Tip Load (lb)	Pitch (deg)	Flapwise Frequency (Hz)	Chordwise Frequency (Hz)
36	4.01	-10.1	0.4687	1.269
37	4.52	-10.1	0.4875	1.094
38	1.5	-15	0.7375	2.788
39	0	-15	4.113	16.48
40	0.49	-15	1.256	4.944
41	1.01	-15	0.8937	3.463
42	2.01	-15	0.6312	2.256
43	3.02	-15	0.5437	1.588
44	3.02	15.04	0.55	1.569
45	2.01	15.04	0.6312	2.25
46	1.5	15.04	0.7375	2.781
47	1.01	15.04	0.8875	3.456
48	0.49	15.04	1.256	4.925
49	0	15.04	4.181	16.48
50	0	30.1	4.131	16.51
51	0	30.1	4.131	16.51
52	0.49	30.1	1.256	4.875
53	1.01	30.1	0.9125	3.313
54	2.01	30.1	0.6937	2.019
55	1.5	30.1	0.775	2.569
56	1.5	44.8	0.8312	2.4
57	1.01	44.8	0.95	3.144
58	0.49	44.8	1.269	4.787
59	0	44.8	4.3	16.39
60	0	59.4	4.194	16.44
61	0.49	59.4	1.288	4.706
62	1.01	59.4	0.9812	3.044
63	1.5	59.4	0.8687	2.319
64	0	75.19	4.119	16.49
65	0.49	75.19	1.294	4.65
66	1.01	75.19	1	2.963
67	1.01	90.1	1	2.944
68	0.49	90.1	1.306	4.631
69	0	90.1	4.138	16.46
70	0.49	10.1	1.256	4.931
71	4.52	10.1	0.4937	1.087
72	4.01	10.1	0.4812	1.213
73	3.02	10.1	0.5	1.694
74	2.01	10.1	0.6125	2.344
75	1.5	10.1	0.725	2.838
76	1.01	10.1	0.8875	3.488

Trial #	Tip Load (lb)	Pitch (deg)	Flapwise Frequency (Hz)	Chordwise Frequency (Hz)
77	0.49	10.1	1.256	4.944
78	0	10.1	4.138	16.44

Table 6 Princeton Beam Data [1:46-50] (Included for Reference)

Tip Load (lb)	Pitch (deg)	Flap Frequency (Hz)	Chord Frequency (Hz)
0	0	4.475	17.217
0	0	4.607	17.213
0	0	4.49	17.171
0	0		17.174
0	0		17.207
0	0	4.464	17.258
1	-105	1.033	3.138
1	-90		3.122
1	-90	1.034	3.12
1	-75	1.028	3.135
1	-60	1.011	3.199
1	-45	0.99	3.298
1	-30	0.961	3.443
1	-15	0.939	3.591
1	0	0.932	3.698
1	0		3.647
1	0	0.935	3.662
1	0	0.928	3.674
1	10	0.935	3.617
1	20	0.945	3.541
1	30	0.96	3.448
1	35		3.394
1	40	0.979	3.354
1	50	0.997	3.277
1	60	1.012	3.215
1	70	1.023	3.175
1	80	1.032	3.145
1	90	1.035	3.143
1	90	1.033	3.138
1	105	1.029	3.155
2	-20	0.682	2.315
2	-10	0.648	2.517
2	0	0.632	2.629
2	0	0.631	2.637

Tip Load (lb)	Pitch (deg)	Flap Frequency (Hz)	Chord Frequency (Hz)
2	5	0.636	2.559
2	10	0.648	2.517
2	15	0.664	2.424
2	20	0.683	2.317
2	25	0.706	2.232
3	-15	0.555	1.723
3	-10	0.514	1.862
3	0	0.462	2.162
3	0	0.461	2.161
3	5	0.478	2.043
3	10	0.515	1.863
3	15	0.553	1.731
4	-5		1.558
4	-5	0.391	1.559
4	0	0.317	1.9
4	5	0.398	1.538
4.5	0	0.199	1.784
4.5	0	0.199	

Table 7 Laser Vibrometer Data, 0 lb Tip Load, 0 degrees Pitch, Mode 1

X Location (in)	Normalized X Location (x/L)	Peak Measured Velocity (m/s)	Normalized Velocity
-0.250	-0.008	1.4174E-06	0.019
1.025	0.034	1.2451E-06	0.016
2.300	0.077	7.5701E-07	0.008
3.575	0.119	2.7077E-07	0.000
4.850	0.162	6.0092E-07	0.005
6.125	0.204	2.2899E-06	0.033
7.400	0.247	4.6158E-06	0.072
8.675	0.289	7.0373E-06	0.112
9.950	0.332	9.2338E-06	0.148
11.213	0.374	1.1329E-05	0.183
12.475	0.416	1.3752E-05	0.223
13.738	0.458	1.6774E-05	0.273
15.000	0.500	2.0333E-05	0.332
16.250	0.542	2.3721E-05	0.388
17.500	0.583	2.6658E-05	0.436
18.750	0.625	2.9669E-05	0.486
20.000	0.667	3.3029E-05	0.542
21.317	0.711	3.6944E-05	0.606

X Location (in)	Normalized X Location (x/L)	Peak Measured Velocity (m/s)	Normalized Velocity
22.633	0.754	4.1328E-05	0.679
23.950	0.798	4.5481E-05	0.748
25.267	0.842	4.9142E-05	0.808
26.583	0.886	5.2700E-05	0.867
27.900	0.930	5.5963E-05	0.921
28.750	0.958	5.8711E-05	0.966
29.600	0.987	6.0750E-05	1.000

Table 8 Laser Vibrometer Data, 0 lb Tip Load, 0 degrees Pitch, Mode 2

X Location (in)	Normalized X Location (x/L)	Peak Measured Velocity (m/s)	Normalized Velocity
-0.250	-0.008	1.1461E-04	0.000
1.025	0.034	5.3323E-04	0.020
2.300	0.077	1.5673E-03	0.070
3.575	0.119	3.1850E-03	0.148
4.850	0.162	5.1853E-03	0.245
6.125	0.204	7.4725E-03	0.356
7.400	0.247	9.7621E-03	0.466
8.675	0.289	1.1949E-02	0.572
9.950	0.332	1.3844E-02	0.664
11.213	0.374	1.5369E-02	0.738
12.475	0.416	1.6313E-02	0.783
13.738	0.458	1.6649E-02	0.799
15.000	0.500	1.6456E-02	0.790
16.250	0.542	1.5866E-02	0.762
17.500	0.583	1.4379E-02	0.690
18.750	0.625	1.2337E-02	0.591
20.000	0.667	9.6408E-03	0.461
21.317	0.711	6.2989E-03	0.299
22.633	0.754	2.4890E-03	0.115
23.950	0.798	1.9169E-03	-0.087
25.267	0.842	6.3166E-03	-0.300
26.583	0.886	1.1172E-02	-0.535
27.900	0.930	1.5735E-02	-0.755
28.750	0.958	1.9113E-02	-0.919
29.600	0.987	2.0798E-02	-1.000

Table 9 Table 5 Laser Vibrometer Data, 0 lb Tip Load, 0 degrees Pitch, Mode 3

X Location (in)	Normalized X Location (x/L)	Peak Measured Velocity (m/s)	Normalized Velocity
-0.300	-0.010	1.2699E-03	0.014
1.025	0.034	4.1388E-03	0.070
2.350	0.078	1.0788E-02	0.198
3.675	0.123	1.9880E-02	0.373
5.000	0.167	2.9268E-02	0.555
6.250	0.208	3.7096E-02	0.706
7.500	0.250	4.2070E-02	0.802
8.750	0.292	4.3382E-02	0.827
10.000	0.333	4.0732E-02	0.776
11.238	0.375	3.4431E-02	0.654
12.475	0.416	2.5078E-02	0.474
13.713	0.457	1.3441E-02	0.249
14.950	0.498	5.3124E-04	0.000
16.213	0.540	1.2400E-02	-0.229
17.475	0.583	2.3799E-02	-0.449
18.738	0.625	3.2345E-02	-0.614
20.000	0.667	3.6952E-02	-0.703
21.250	0.708	3.7084E-02	-0.705
22.500	0.750	3.2882E-02	-0.624
23.750	0.792	2.4269E-02	-0.458
25.000	0.833	1.0666E-02	-0.196
26.525	0.884	8.0406E-03	0.145
28.050	0.935	2.7609E-02	0.523
28.875	0.963	4.3372E-02	0.827
29.700	0.990	5.2345E-02	1.000

Table 10 Table 5 Laser Vibrometer Data, 1 lb Tip Load, 0 degrees Pitch, Mode 1

X Location (in)	Normalized X Location (x/L)	Peak Measured Velocity (m/s)	Normalized Velocity
-0.200	-0.007	1.1557E-06	0.000
1.088	0.036	4.0992E-06	0.004
2.375	0.079	1.1724E-05	0.015
3.663	0.122	2.4077E-05	0.033
4.950	0.165	4.0614E-05	0.057
6.188	0.206	6.0604E-05	0.086
7.425	0.248	8.4086E-05	0.120
8.663	0.289	1.1076E-04	0.158
9.900	0.330	1.3893E-04	0.199

X Location (in)	Normalized X Location (x/L)	Peak Measured Velocity (m/s)	Normalized Velocity
11.150	0.372	1.6933E-04	0.243
12.400	0.413	2.0203E-04	0.290
13.650	0.455	2.3583E-04	0.339
14.900	0.497	2.7064E-04	0.389
16.175	0.539	3.0822E-04	0.443
17.450	0.582	3.4825E-04	0.501
18.725	0.624	3.8635E-04	0.556
20.000	0.667	4.2376E-04	0.610
21.250	0.708	4.6008E-04	0.663
22.500	0.750	4.9571E-04	0.714
23.750	0.792	5.3010E-04	0.764
25.000	0.833	5.6760E-04	0.818
26.500	0.883	6.1489E-04	0.886
28.000	0.933	6.5442E-04	0.943
28.675	0.956	6.7393E-04	0.972
29.350	0.978	6.9364E-04	1.000

Table 11 Table 5 Laser Vibrometer Data, 1 lb Tip Load, 0 degrees Pitch, Mode 2

X Location (in)	Normalized X Location (x/L)	Peak Measured Velocity (m/s)	Normalized Velocity
-0.200	-0.007	2.7907E-04	0.000
1.088	0.036	1.0796E-03	0.019
2.375	0.079	3.0618E-03	0.065
3.663	0.122	6.0668E-03	0.134
4.950	0.165	9.9219E-03	0.224
6.188	0.206	1.4240E-02	0.324
7.425	0.248	1.8750E-02	0.429
8.663	0.289	2.3165E-02	0.532
9.900	0.330	2.7687E-02	0.637
11.150	0.372	3.2074E-02	0.739
12.400	0.413	3.5823E-02	0.826
13.650	0.455	3.8690E-02	0.892
14.900	0.497	4.1119E-02	0.949
16.175	0.539	4.2846E-02	0.989
17.450	0.582	4.3324E-02	1.000
18.725	0.624	4.2266E-02	0.975
20.000	0.667	4.0451E-02	0.933
21.250	0.708	3.8257E-02	0.882
22.500	0.750	3.4760E-02	0.801

X Location (in)	Normalized X Location (x/L)	Peak Measured Velocity (m/s)	Normalized Velocity
23.750	0.792	3.0307E-02	0.698
25.000	0.833	2.4807E-02	0.570
26.500	0.883	1.7860E-02	0.408
28.000	0.933	1.1007E-02	0.249
28.675	0.956	6.3454E-03	0.141
29.350	0.978	4.0072E-03	0.087

Table 12 Table 5 Laser Vibrometer Data, 1 lb Tip Load, 0 degrees Pitch, Mode 3

X Location (in)	Normalized X Location (x/L)	Peak Measured Velocity (m/s)	Normalized Velocity
-0.250	-0.008	7.2170E-04	0.000
1.050	0.035	2.2832E-03	0.051
2.350	0.078	5.9509E-03	0.170
3.650	0.122	1.1158E-02	0.339
4.950	0.165	1.6941E-02	0.526
6.200	0.207	2.2439E-02	0.705
7.450	0.248	2.7012E-02	0.853
8.700	0.290	3.0172E-02	0.956
9.950	0.332	3.1537E-02	1.000
11.213	0.374	3.0880E-02	0.979
12.475	0.416	2.8172E-02	0.891
13.738	0.458	2.3560E-02	0.741
15.000	0.500	1.7377E-02	0.540
16.238	0.541	1.0106E-02	0.305
17.475	0.583	2.2839E-03	0.051
18.713	0.624	5.5128E-03	-0.155
19.950	0.665	1.2704E-02	-0.389
21.213	0.707	1.8738E-02	-0.585
22.475	0.749	2.3064E-02	-0.725
23.738	0.791	2.5205E-02	-0.795
25.000	0.833	2.4662E-02	-0.777
26.500	0.883	2.0800E-02	-0.652
28.000	0.933	1.5106E-02	-0.467
28.650	0.955	1.0239E-02	-0.309
29.300	0.977	7.4993E-03	-0.220

Table 13 Table 5 Laser Vibrometer Data, 2 lb Tip Load, 0 degrees Pitch, Mode 1

X Location (in)	Normalized X Location (x/L)	Peak Measured Velocity (m/s)	Normalized Velocity
-0.250	-0.008	8.9827E-07	0.001
1.050	0.035	6.5411E-07	0.000
2.350	0.078	2.4819E-06	0.008
3.650	0.122	5.6369E-06	0.022
4.950	0.165	9.5163E-06	0.040
6.200	0.207	1.4183E-05	0.060
7.450	0.248	1.9925E-05	0.086
8.700	0.290	2.6178E-05	0.114
9.950	0.332	3.3611E-05	0.147
11.213	0.374	4.2081E-05	0.185
12.475	0.416	5.0371E-05	0.222
13.738	0.458	6.0545E-05	0.267
15.000	0.500	7.3809E-05	0.326
16.250	0.542	8.7979E-05	0.390
17.500	0.583	1.0127E-04	0.449
18.750	0.625	1.1314E-04	0.502
20.000	0.667	1.2376E-04	0.549
21.250	0.708	1.3678E-04	0.608
22.500	0.750	1.5208E-04	0.676
23.750	0.792	1.6593E-04	0.738
25.000	0.833	1.7893E-04	0.796
26.500	0.883	1.9403E-04	0.863
28.000	0.933	2.0880E-04	0.929
28.725	0.958	2.1853E-04	0.972
29.450	0.982	2.2473E-04	1.000

Table 14 Table 5 Laser Vibrometer Data, 2 lb Tip Load, 0 degrees Pitch, Mode 2

X Location (in)	Normalized X Location (x/L)	Peak Measured Velocity (m/s)	Normalized Velocity
-0.250	-0.008	9.1959E-05	0.000
1.050	0.035	2.0644E-04	0.017
2.350	0.078	4.9252E-04	0.060
3.650	0.122	9.3891E-04	0.128
4.950	0.165	1.5055E-03	0.213
6.200	0.207	2.1536E-03	0.310
7.450	0.248	2.8447E-03	0.415
8.700	0.290	3.5361E-03	0.519
9.950	0.332	4.1958E-03	0.618

X Location (in)	Normalized X Location (x/L)	Peak Measured Velocity (m/s)	Normalized Velocity
11.213	0.374	4.8174E-03	0.712
12.475	0.416	5.3997E-03	0.799
13.738	0.458	5.9151E-03	0.877
15.000	0.500	6.3200E-03	0.938
16.250	0.542	6.5956E-03	0.979
17.500	0.583	6.7329E-03	1.000
18.750	0.625	6.7113E-03	0.997
20.000	0.667	6.5340E-03	0.970
21.250	0.708	6.2085E-03	0.921
22.500	0.750	5.7339E-03	0.850
23.750	0.792	5.0613E-03	0.748
25.000	0.833	4.1154E-03	0.606
26.500	0.883	2.9846E-03	0.436
28.000	0.933	1.9751E-03	0.284
28.725	0.958	1.2459E-03	0.174
29.450	0.982	8.3436E-04	0.112

Table 15 Table 5 Laser Vibrometer Data, 3 lb Tip Load, 0 degrees Pitch, Mode 3

X Location (in)	Normalized X Location (x/L)	Peak Measured Velocity (m/s)	Normalized Velocity
-0.250	-0.008	2.9321E-04	0.095
1.050	0.035	3.9822E-04	0.144
2.350	0.078	6.1935E-04	0.246
3.650	0.122	9.1510E-04	0.383
4.950	0.165	1.2386E-03	0.533
6.200	0.207	1.5507E-03	0.678
7.450	0.248	1.8256E-03	0.805
8.700	0.290	2.0428E-03	0.906
9.950	0.332	2.1867E-03	0.972
11.213	0.374	2.2468E-03	1.000
12.475	0.416	2.2162E-03	0.986
13.738	0.458	2.0941E-03	0.929
15.000	0.500	1.8853E-03	0.833
16.250	0.542	1.5990E-03	0.700
17.500	0.583	1.2516E-03	0.539
18.750	0.625	8.6458E-04	0.360
20.000	0.667	4.6614E-04	0.176
21.250	0.708	8.7025E-05	0.000
22.500	0.750	2.5617E-04	-0.078

X Location (in)	Normalized X Location (x/L)	Peak Measured Velocity (m/s)	Normalized Velocity
23.750	0.792	5.2939E-04	-0.205
25.000	0.833	7.0606E-04	-0.287
26.500	0.883	7.4775E-04	-0.306
28.000	0.933	6.5659E-04	-0.264
28.725	0.958	4.9568E-04	-0.189
29.450	0.982	3.6861E-04	-0.130

Table 16 Table 5 Laser Vibrometer Data, 3 lb Tip Load, 0 degrees Pitch, Mode 1

X Location (in)	Normalized X Location (x/L)	Peak Measured Velocity (m/s)	Normalized Velocity
-0.350	-0.012	1.3948E-06	0.000
0.963	0.032	5.7544E-06	0.002
2.275	0.076	1.8832E-05	0.008
3.588	0.120	4.3132E-05	0.019
4.900	0.163	7.7915E-05	0.036
6.150	0.205	1.2241E-04	0.056
7.400	0.247	1.7799E-04	0.082
8.650	0.288	2.4472E-04	0.113
9.900	0.330	3.2137E-04	0.148
11.175	0.373	4.0743E-04	0.188
12.450	0.415	5.0305E-04	0.233
13.725	0.458	6.0548E-04	0.280
15.000	0.500	7.1092E-04	0.329
16.250	0.542	8.2756E-04	0.383
17.500	0.583	9.5921E-04	0.444
18.750	0.625	1.0936E-03	0.507
20.000	0.667	1.2282E-03	0.569
21.250	0.708	1.3693E-03	0.635
22.500	0.750	1.5046E-03	0.697
23.750	0.792	1.6296E-03	0.755
25.000	0.833	1.7831E-03	0.827
26.475	0.883	1.9561E-03	0.907
27.950	0.932	2.0693E-03	0.959
28.650	0.955	2.1209E-03	0.983
29.350	0.978	2.1568E-03	1.000

Table 17 Table 5 Laser Vibrometer Data, 3 lb Tip Load, 0 degrees Pitch, Mode 2

X Location (in)	Normalized X Location (x/L)	Peak Measured Velocity (m/s)	Normalized Velocity
-0.350	-0.012	1.2320E-06	0.000
0.963	0.032	2.0582E-06	0.005
2.275	0.076	7.6108E-06	0.039
3.588	0.120	1.7825E-05	0.102
4.900	0.163	3.0743E-05	0.181
6.150	0.205	4.5094E-05	0.269
7.400	0.247	5.8888E-05	0.354
8.650	0.288	7.6101E-05	0.460
9.900	0.330	9.2663E-05	0.562
11.175	0.373	1.0822E-04	0.657
12.450	0.415	1.2786E-04	0.778
13.725	0.458	1.3958E-04	0.850
15.000	0.500	1.4916E-04	0.909
16.250	0.542	1.6103E-04	0.981
17.500	0.583	1.6382E-04	0.999
18.750	0.625	1.6402E-04	1.000
20.000	0.667	1.6405E-04	1.000
21.250	0.708	1.5712E-04	0.957
22.500	0.750	1.4371E-04	0.875
23.750	0.792	1.2536E-04	0.762
25.000	0.833	1.0727E-04	0.651
26.475	0.883	8.3764E-05	0.507
27.950	0.932	5.3506E-05	0.321
28.650	0.955	3.2464E-05	0.192
29.350	0.978	2.4487E-05	0.143

Table 18 Table 5 Laser Vibrometer Data, 3 lb Tip Load, 0 degrees Pitch, Mode 3

X Location (in)	Normalized X Location (x/L)	Peak Measured Velocity (m/s)	Normalized Velocity
-0.350	-0.012	1.4732E-06	0.000
0.963	0.032	2.4664E-06	-0.006
2.275	0.076	5.8784E-06	0.028
3.588	0.120	1.3234E-05	0.074
4.900	0.163	2.5357E-05	0.151
6.150	0.205	4.2107E-05	0.257
7.400	0.247	6.2593E-05	0.386
8.650	0.288	8.4734E-05	0.526
9.900	0.330	1.0602E-04	0.660

X Location (in)	Normalized X Location (x/L)	Peak Measured Velocity (m/s)	Normalized Velocity
11.175	0.373	1.2486E-04	0.779
12.450	0.415	1.4112E-04	0.882
13.725	0.458	1.5391E-04	0.962
15.000	0.500	1.5986E-04	1.000
16.250	0.542	1.5781E-04	0.987
17.500	0.583	1.5070E-04	0.942
18.750	0.625	1.4030E-04	0.877
20.000	0.667	1.2479E-04	0.779
21.250	0.708	1.0317E-04	0.642
22.500	0.750	7.9362E-05	0.492
23.750	0.792	5.8890E-05	0.363
25.000	0.833	4.0364E-05	0.246
26.475	0.883	1.9204E-05	0.112
27.950	0.932	6.4174E-06	0.031
28.650	0.955	6.4250E-06	-0.031
29.350	0.978	8.4416E-06	-0.044

Table 19 Laser Vibrometer Natural Frequency Values

Tip Load (lb)	Pitch Angle (deg)	Frequency Mode 1 (Hz)	Frequency Mode 2 (Hz)	Frequency Mode 3 (Hz)
0	0	4.500	27.38	76.50
1.01	0	0.875	18.25	54.38
2.01	0	0.5983	16.13	36.53
3.02	0	0.4219	14.06	33.95

Appendix B. Linear Theory [6]

The following derivation of the linear beam theory used for mode shape comparisons has been reproduced in its entirety. None of it is original work for this thesis.

Cantilever Beam with an End Mass

Eigenvalue problem

$$\left[EI(x)Y''(x)\right]'' = \omega^2 m(x)Y(x)$$

Boundary conditions

$$Y(x)\Big|_{x=0} = 0$$

$$Y'(x)\Big|_{x=0} = 0$$

$$\left[EI(x)Y''(x)\right]\Big|_{x=L} = 0$$

$$\left\{-\left[EI(x)Y''(x)\right]'\right\}\Big|_{x=L} = \left[\omega^2 MY(x)\right]\Big|_{x=L}$$

Uniform cantilever beam ($m(x)=m$, $EI(x)=EI$)

$$Y^{IV}(x) = \frac{\omega^2 m}{EI}Y(x) = \beta^4 Y(x); \quad \beta^4 = \frac{\omega^2 m}{EI}$$

$$Y(0) = 0$$

$$Y'(0) = 0$$

$$Y''(L) = 0$$

$$Y'''(L) + \frac{\omega^2 M}{EI}Y(L) = Y'''(L) + \beta^4 \frac{M}{m}Y(L) = 0$$

Solution of the eigenvalue problem

$$Y(x) = A\sin\beta x + B\cos\beta x + C\sinh\beta x + D\cosh\beta x$$

$$Y(0) = B + D = 0$$

$$D = -B$$

$$Y'(0) = \beta(A + C) = 0$$

$$C = -A$$

$$Y(x) = A(\sin\beta x - \sinh\beta x) + B(\cos\beta x - \cosh\beta x)$$

$$Y''(L) = -\beta^2\left[A(\sin\beta L + \sinh\beta L) + B(\cos\beta L + \cosh\beta L)\right] = 0$$

$$B = -A\frac{\sin\beta L + \sinh\beta L}{\cos\beta L + \cosh\beta L}$$

$$Y(x) = A\left[(\sin\beta x - \sinh\beta x) - \frac{\sin\beta L + \sinh\beta L}{\cos\beta L + \cosh\beta L}(\cos\beta x - \cosh\beta x)\right]$$

$$-A\beta^3\left[(\cos\beta L + \cosh\beta L) + \frac{\sin\beta L + \sinh\beta L}{\cos\beta L + \cosh\beta L}(\sin\beta L - \sinh\beta L)\right]$$

$$+ A\beta^4\frac{M}{m}\left[(\sin\beta L - \sinh\beta L) - \frac{\sin\beta L + \sinh\beta L}{\cos\beta L + \cosh\beta L}(\cos\beta L - \cosh\beta L)\right] = 0$$

Characteristic equation

$$-(\cos^2\beta L + 2\cos\beta L\cosh\beta L + \cosh^2\beta L) - (\sin^2\beta L - \sinh^2\beta L)$$

$$+\beta\frac{M}{m}(\sin\beta L\cos\beta L + \sin\beta L\cosh\beta L - \cos\beta L\sinh\beta L - \sinh\beta L\cosh\beta L)$$

$$-\beta\frac{M}{m}(\sin\beta L\cos\beta L - \sin\beta L\cosh\beta L + \cos\beta L\sinh\beta L - \sinh\beta L\cosh\beta L) = 0$$

$$\beta L\frac{M}{mL}(\sin\beta L\cosh\beta L - \cos\beta L\sinh\beta L) - (1 + \cos\beta L\cosh\beta L) = 0$$

Solve the characteristic equation using Mathematica, Matlab, or Mathcad (see Mathematica output).

$$\omega = (\beta L)^2\sqrt{\frac{EI}{mL^4}}$$

Modeshapes

$$Y(x) = A\left[(\sin\beta L\bar{x} - \sinh\beta L\bar{x}) - \frac{\sin\beta L + \sinh\beta L}{\cos\beta L + \cosh\beta L}(\cos\beta L\bar{x} - \cosh\beta L\bar{x})\right]; \quad \bar{x} = \frac{x}{L}$$

Bibliography

[1] Dowell, E. H. and Traybar, J. *An Experimental Study of the Nonlinear Stiffness of a Rotor Blade Undergoing Flap, Lag, and Twist Deformations, AMS Report No. 1194, January 1975*. Contract NAS 2-7615. U.S. Army Air Mobility Research and Development Laboratory: Ames Research Center, January 1975 (NASA CR-137968).

[2] Hopkins, A. Stewart and Ormistion, Robert A. "An Examination of Selected Problems in Rotor Blade Structural mechanics and Dynamics," *Presented at the American Helicopter Society 59th Annual Forum, Phoenix, Arizona.* May, 2003.

[3] Dowell, E. H., Traybar, J., and Hodges, D. H. "An Experimental-Theoretical Correlation Study of Nonlinear Bending and Torsion Deformation of a Cantilever Beam," *Journal of Sound and Vibration*, vol. 50, no. 4, Feb. 22, 1977, pp. 533 - 544.

[4] Matweb material property Data. http://www.matweb.com/search/SpecificMaterial.asp?bassnum=MA7075T6 27 April 2006.

[5] Dowell, E. H. and Traybar, J. *An Addendum to AMS Report No 1194 Entitled An Experimental Study of the Nonlinear Stiffness of a Rotor Blade Undergoing Flap, Lag, and Twist Deformations, AMS Report No. 1257, December 1975*. U.S. Army Air Mobility Research and Development Laboratory: Ames Research Center, December 1975 (NASA CR-137969).

[6] Kunz, Donald L. Associate Professor of Aerospace Engineering, Air Force Institute of Technology “Cantilever Beam with Tip Mass.” Electronic Message. 8 March 2006.

Vita

Captain Michael S. Whiting graduated from Miami Sunset Senior High School in Miami, Florida. He attended undergraduate studies at the United States Air Force Academy in Colorado Springs, Colorado where he graduated with dual Bachelor of Sciences degrees in Mechanical Engineering and Engineering Mechanics and a commission in the United States Air Force in 2002. He was married in May 2002 and has one child.

His first assignment was at Wright-Patterson Air Force Base as a project engineer in the Propulsion Program Office in August 2002. In August 2004, he entered the Graduate School of Engineering and Management, Air Force Institute of Technology. Following his time at AFIT he has been assigned to the Navstar Global Positioning System Joint Program Office at Los Angeles Air Force Base in El Segundo, California.

REPORT DOCUMENTATION PAGE

Form Approved
OMB No. 074-0188

1. REPORT DATE *(DD-MM-YYYY)*	**2. REPORT TYPE**	**3. DATES COVERED** *(From – To)*
13-06-2006	**Master's Thesis**	Mar 2003 – Jun 2006

4. TITLE AND SUBTITLE

Dynamic Nonlinear Bending and Torsion of a Cantilever Beam

5a. CONTRACT NUMBER

5b. GRANT NUMBER

5c. PROGRAM ELEMENT NUMBER

6. AUTHOR(S)

Whiting, Michael, S., Lieutenant, USAF

5d. PROJECT NUMBER

5e. TASK NUMBER

5f. WORK UNIT NUMBER

7. PERFORMING ORGANIZATION NAMES(S) AND ADDRESS(S)
Air Force Institute of Technology
Graduate School of Engineering and Management (AFIT/EN)
2950 Hobson Way
WPAFB OH 45433-7765

8. PERFORMING ORGANIZATION REPORT NUMBER

AFIT/GAE/ENY/06-M32

9. SPONSORING/MONITORING AGENCY NAME(S) AND ADDRESS(ES)
Dr. Robert A. Ormiston
U.S. Army Aeroflightdynamics Directorate
NASA Ames Research Center, MS 215-1
Moffett Field, CA 94035-1000 Phone: 650-604-5000

10. SPONSOR/MONITOR'S ACRONYM(S)

11. SPONSOR/MONITOR'S REPORT NUMBER(S)

12. DISTRIBUTION/AVAILABILITY STATEMENT
APPROVED FOR PUBLIC RELEASE; DISTRIBUTION UNLIMITED.

13. SUPPLEMENTARY NOTES

14. ABSTRACT

This effort sought to measure the dynamic nonlinear bending and torsion response of a cantilever beam. The natural frequencies of a cantilever beam in both chord and flap directions were measured at different static root pitch angles with varying levels of weights attached at the free end. The results were compared with previous experimentation to validate the data and testing procedures while lowering the associated error bands. Additionally, methodology for measuring mode shapes was set forth and mode shapes were measured for a few test cases with zero degrees of root pitch.

15. SUBJECT TERMS
Cantilever Beam, Modal Analysis, Natural Frequency, Pitch (Inclination), Tip Load, Dynamic Response

16. SECURITY CLASSIFICATION OF: U			**17. LIMITATION OF ABSTRACT**	**18. NUMBER OF PAGES**	**19a. NAME OF RESPONSIBLE PERSON**
REPORT	**ABSTRACT**	**c. THIS PAGE**			Donald L. Kunz (ENY)
U	**U**	**U**	**UU**	**63**	**19b. TELEPHONE NUMBER** *(Include area code)* (937) 785-3636, ext 4320; e-mail: Donald.Kunz@afit.edu

Standard Form 298 (Rev: 8-98)
Prescribed by ANSI Std. Z39-18